Bioorganic & Medicinal Chemistry 24 (2016) 1520–1527

Contents lists available at ScienceDirect

Bioorganic & Medicinal Chemistry

journal homepage: www.elsevier.com/locate/bmc

Efficacy of peptide nucleic acid and selected conjugates against specific cellular pathologies of amyotrophic lateral sclerosis

Elisse C. Browne [a], Sonam Parakh [b,d], Luke F. Duncan [a], Steven J. Langford [c], Julie D. Atkin [b,d], Belinda M. Abbott [a,*]

[a] Department of Chemistry and Physics, La Trobe Institute for Molecular Science, La Trobe University, Melbourne 3086, Australia
[b] Department of Biochemistry and Genetics, La Trobe Institute for Molecular Science, La Trobe University, Melbourne 3086, Australia
[c] School of Chemistry, Monash University, Clayton 3800, Australia
[d] Department of Biomedical Sciences, Faculty of Medicine and Health Science, Macquarie University, Sydney 2109, Australia

ARTICLE INFO

Article history:
Received 14 December 2015
Revised 9 February 2016
Accepted 17 February 2016
Available online 18 February 2016

Keywords:
Peptide nucleic acid
Amyotrophic lateral sclerosis
Vitamin conjugation

ABSTRACT

Cellular studies have been undertaken on a nonamer peptide nucleic acid (PNA) sequence, which binds to mRNA encoding superoxide dismutase 1, and a series of peptide nucleic acids conjugated to synthetic lipophilic vitamin analogs including a recently prepared menadione (vitamin K) analog. Reduction of both mutant superoxide dismutase 1 inclusion formation and endoplasmic reticulum stress, two of the key cellular pathological hallmarks in amyotrophic lateral sclerosis, by two of the prepared PNA oligomers is reported for the first time.

1. Introduction

Amyotrophic lateral sclerosis (ALS) is a fatal neurodegenerative disorder which affects the upper and lower motor neurons of the brain, brain stem and spinal cord.[1] It causes progressive muscle weakness, paralysis and death within 3–5 years of diagnosis and there is currently no effective treatment. Around 10% of ALS cases are familial (fALS), caused by genetic mutations. However, the majority of ALS (90%) is sporadic, with no previous family history.[2] Mutations in the superoxide dismutase 1 (SOD1) gene account for approximately 20% of familial ALS cases and the most common mutation in North America is A4V (alanine to valine).[3,4] SOD1 is a major cytosolic protein which catalyzes the reduction of harmful, free superoxide radicals into molecular oxygen and hydrogen peroxide.

The etiology of ALS remains unclear but the formation of intracellular ubiquitin-positive inclusions containing misfolded proteins is a characteristic pathological hallmark.[5] Misfolded SOD1 inclusions are present in both sporadic human[6] and familial ALS patients, as well as transgenic SOD1^{G93A} mice,[7] the most widely used animal disease model in preclinical studies. Stress in the endoplasmic reticulum (ER) is also recognized to be an important pathway to motor neuron death in ALS. ER stress is triggered when misfolded proteins accumulate within the ER. This triggers the unfolded protein response (UPR), a signaling pathway that aims to relieve the stress and thus restore homeostasis. However if ER stress is prolonged, apoptosis is triggered. The transition of UPR from cell survival to cell death is mediated by CCAAT-enhancer binding protein homologous protein (CHOP),[8] a transcription factor which translocates to the nucleus when activated. We and others previously demonstrated that ER stress is present in sporadic ALS patient tissues[9] as well as in cells expressing mutant SOD1 and transgenic SOD1^{G93A} mice.[10–14] Novel pharmacological agents that prevent the formation of misfolded mutant SOD1 inclusions and inhibit the activation of CHOP in cells expressing mutant SOD1, and hence the pro-apoptotic phase of UPR, would therefore have therapeutic application in ALS.

Antisense agents such as peptide nucleic acids (PNA) are short single stranded nucleic acid analogs designed to specifically bind to complementary messenger ribonucleic acid (mRNA) targets through Watson and Crick hydrogen bonding. As a result, these antisense agents can silence a particular gene of interest. PNA is a third generation oligonucleotide, which replaces the traditional phosphate backbone of RNA/DNA with a peptide backbone made up of repeating *N*-(2-aminoethyl)glycine units and the sugar moiety replaced with a methylene carbonyl linker where the nucleic bases are attached (Fig. 1).

The modified backbone of PNA gives rise to resistance to enzymatic degradation and leads to higher affinity binding, rates of

* Corresponding author.
E-mail address: b.abbott@latrobe.edu.au (B.M. Abbott).

http://dx.doi.org/10.1016/j.bmc.2016.02.022
0968-0896/

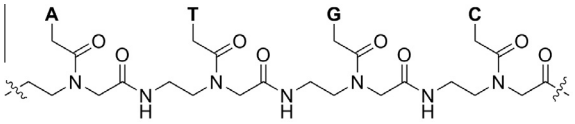

Figure 1. General structure of peptide nucleic acid (PNA) containing the four nucleobases of adenine (A), thymine (T), guanine (G) and cytosine (C).

association and subsequently an increase in duplex stability as there are no repulsive electrostatic interactions.[15] Additionally, the neutrality of the backbone significantly reduces the chance of undesired nonspecific interactions such as binding to cellular proteins.[16] PNA exhibits low toxicity in cells and is stable of a wide pH range, particularly toward the acidic end of the scale where DNA can be denatured.

The major limitation of PNA as an efficient antisense drug is its low phospholipid solubility due to the hydrophilic nature of the molecule, PNA does not readily cross cell membranes. Hydrophobic vitamins such as vitamin K and vitamin E are hypothesized as good candidates for conjugation to PNA. The main function of vitamin K is post-translational modification during the biosynthesis of vitamin K dependent proteins.[17] The synthetic form of this vitamin, vitamin K3 (menadione) has been found to readily cross the blood brain barrier as it is a small lipophilic molecule.[18] Despite its larger size, highly lipophilic vitamin E (tocopherol) has also been found to cross the blood brain barrier.[19] While the main task of this vitamin is as an antioxidant, vitamin E has also been shown to alleviate oxidative stress by promoting normal cell function.[20]

We have previously described the synthesis and conjugation of tocopherol (vitamin E) analogs to PNA for the investigation of effects on hybridization.[21] In this further study, we present the synthesis of a menadione (vitamin K) analog, its conjugation to the same nine nucleobase PNA oligomer and the subsequent hybridization results. In addition, this novel vitamin K conjugated oligomer, along with the previously synthesized three vitamin E derived conjugated PNA oligomers and the unconjugated PNA oligomer, were studied using cellular assays to determine their effects on the formation of mutant SOD1 inclusions and induction of on ER stress.

2. Results and discussion

2.1. Synthesis and thermodynamic studies of the menadione-PNA conjugate

The menadione analog was synthesized by the adaptation of the methods of Abell et al.[22] Commercially available menadione was directly brominated using molecular bromine in the presence of sodium acetate and glacial acetic acid to yield the brominated adduct **1**,[23] followed by reduction of the dione using potassium hydroxide and in situ methylation with dimethyl sulfate to give **2** in 45% yield over the two steps (Scheme 1). Alkylation of **2** using ethyl bromoacetate was achieved via a copper transmetalation reaction through a diaryl cuprate intermediate from treatment with *n*-butyllithium and copper bromide dimethyl sulfide. Increasing the number of equivalents of ethyl bromoacetate from 1.1 to 1.5 and extending the reaction time from 5 to 18 h resulted in an optimized yield of 55%, a considerable improvement over the previously reported 34% yield for this step.[22] Reduction of the ethyl ester **3** using lithium aluminum hydride proceeded in high yield to give the corresponding alcohol **4** which was succinylated using the anhydride to afford **5**. Ceric ammonium nitrate (CAN) was utilized to oxidatively deprotect the methoxy groups and restore the quinone functionality that is characteristic of the vitamin K family affording **6** in 84% yield.

Automated PNA synthesis was performed on PAL resin using standard protocols[24] and two PNA sequences were prepared as previously described: H-GCACGACTT-NH_2 (**PNA1**) and the complementary sequence H-AAGTCGTGC-NH_2 (**PNA2**).[21] Coupling of the menadione analog **6** to the growing oligomer of **PNA1** was then undertaken using the same automated synthetic protocols. Purification by reverse-phase high performance liquid chromatography (RP-HPLC) gave the desired menadione-PNA conjugated oligomer of **6-PNA1** (Fig. 2). Characterization was undertaken using MALDI-TOF mass spectrometry where *m*/*z* calculated for $C_{119}H_{150}N_{55}O_{33}$ requires $[M+H]^+$ 2734.069 and *m*/*z* of $[M+H]^+$ 2734.375 was found.

In order to determine the suitability of the conjugated menadione-PNA oligomer **6-PNA1**, the thermodynamics of hybridization to both the complementary PNA (**PNA2**) and DNA oligomers was undertaken to ensure conjugation did not impair hybridization (Tables 1 and 2). Two complementary methods were chosen for thermodynamic analysis of the duplexes, UV monitored melting curves (UVM)[25,26] and isothermal titration calorimetry (ITC).[27] Data for the control duplexes of **PNA1**/**PNA2** and **PNA1**/DNA was previously recorded[21] and is provided here to facilitate the comparison of the data obtained with the conjugated duplexes. The change in the thermodynamic differences between the two methods agree well with each other.

In the case for both conjugated duplexes, conjugation of the menadione analog does not appear to significantly affect the stability of the duplexes as reflected in the recorded thermal melting temperature (T_m). As expected, lower thermal stability and thus affinity was observed for the mixed duplexes of PNA and DNA oligomers.[28,29] However, the duplex binding affinity, which is related to the enthalpy change (ΔH°) is reduced in both of the conjugated duplexes to the same extent (approximately 73 kJ mol^{-1} on average). As a result of this, the free energy (ΔG°) is also reduced leading to less favorable duplex formation at 37 °C with the conjugated duplex despite no change in T_m. The reduction in ΔH° indicates that there is a weaker interaction between the two oligomers, most likely a result of steric bulk minimizing the interaction of the base pairs adjacent to the conjugate. However, the conformations of the base pairs or stacking patterns may also have an effect along with counter ion uptake and release and hydration factors may also have an effect. Despite the change in the enthalpy and free energy change for this duplex, the thermal melting temperature remains relatively unaffected overall.

2.2. PNA1, 6-PNA1 and 7-PNA1 inhibit the formation of mutant SOD1 inclusions in neuronal cell lines

We next examined the effect of the PNA compounds in cells expressing mutant SOD1 A4V. Mouse neuronal Neuro2a cells were transfected with a previously generated construct encoding SOD1 A4V,[30] tagged with Enhanced Green Fluorescent protein (EGFP) to aid in visualizing the expressed protein. We previously demonstrated that the presence of the EGFP tag does not affect the activity of the protein.[30] Cells were also treated 4 h post transfection either with dimethyl sulfoxide (DMSO) vehicle as a negative control, unconjugated PNA (**PNA1** or its complementary sequence **PNA2**), menadione-conjugate **6-PNA1** (Fig. 2), previously prepared vitamin E derived-conjugates **7- PNA1**, **8-PNA1** and **9-PNA1** (Fig. 3),[21] or (+/−)-*trans*-1,2-bis(2-mercaptoacetamido)cyclohexane (BMC), which we previously demonstrated significantly reduces the formation of mutant SOD1 A4V inclusions and reduced ER stress.[13]

Cells were transfected for 72 h and then examined by fluorescent microscopy with the percentage of cells bearing fluorescent green mutant SOD1 inclusions quantified. Untransfected cells (UTR) were included as a negative control to specifically determine

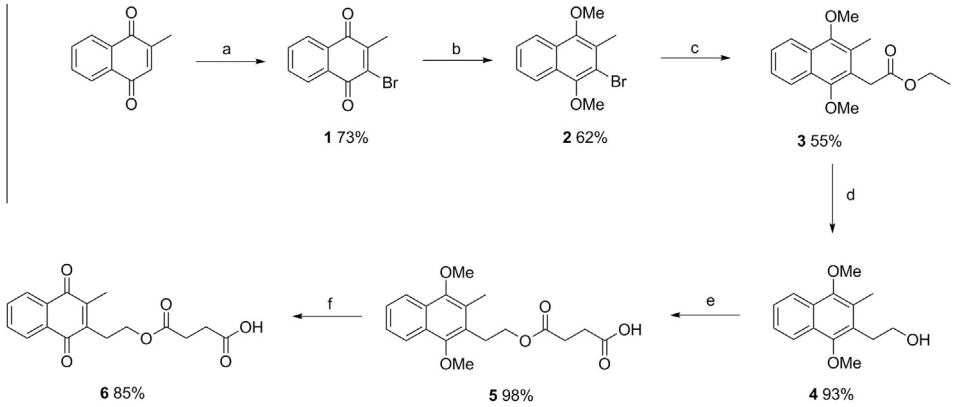

Scheme 1. Synthesis of a menadione analog. Reactions and conditions: (a) Br_2, sodium acetate, glacial acetic acid, 3 days; (b) tetrabutylammonium iodide, tetrahydrofuran/H_2O (3:1), 2.2 M $Na_2S_2O_4$(aq), 20 min then KOH, $(CH_3O)_2SO_2$, 12 h; (c) *n*-butyllithium in hexanes, diethyl ether, 0 °C, 30 min then CuBr·MeS, 2.5 h then $BrCH_2COOCH_2CH_3$, 0 °C, 2 h; (d) $LiAlH_4$, diethyl ether, 35 min; (e) triethylamine, succinic anhydride, 4-(dimethylamino)pyridine, CH_2Cl_2, 12 h; (f) CAN, CH_3CN/H_2O (3:2), 0 °C, 30 min then room temperature, 20 min.

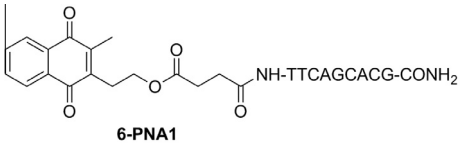

Figure 2. Conjugated menadione-PNA oligomer of **6-PNA1**.

the effects of transfection with mutant SOD1 and, as expected, rarely formed inclusions. However, in control DMSO only treated populations, 19% of transfected cells formed inclusions (Fig. 4A and B, additional low magnification images provided as Supplementary material) similar to our previous observations.[30] As in an earlier study, treatment with BMC significantly reduced the percentage of cells bearing inclusions to 14% compared to DMSO treated cells (p <0.05). Moreover, treatment of SOD1 A4V expressing cells with **6-PNA1** significantly decreased the percentage of cells bearing inclusions to 15% (p <0.05). Furthermore, treatment of cells with **PNA1** and **7-PNA1** significantly reduced the percentage of transfected cells bearing inclusions from 21% in DMSO treated cells to 11% (p <0.01) and 14% (p <0.05) respectively (Fig. 4A and C). There was a slight decrease in inclusion formation in cells treated with compounds **8-PNA1** (17%) and **9-PNA1** (16%), but this was not statistically significant. In contrast, treatment with the negative control PNA, **PNA2**, did not alter the percentage of cells bearing inclusions (20%) as expected. Hence this data indicates that compounds **PNA1**, **6-PNA1** and **7-PNA1** were all equally effective as BMC in preventing the formation of mutant SOD1 inclusions in neuronal cells, the characteristic pathological hallmark of ALS.

2.3. PNA1 and 6-PNA1 reduces ER stress in neuronal cells expressing mutant SOD1 A4V

Since **PNA1**, **6-PNA1** and **7-PNA1** reduced inclusion formation, we proceeded to investigate whether the PNA oligomers could inhibit ER stress induced by mutant SOD1 A4V. We examined the pro-apoptotic phase of UPR using nuclear immunoreactivity to CHOP, as previously described.[13] Neuro2a cells were transfected with the SOD1 A4V-EGFP construct and at 72 h post transfection, cells were fixed and immunocytochemistry for CHOP was performed. Activation of CHOP, indicated by immunoreactivity in the nucleus, was observed in 35% of transfected control cells that were treated with DMSO only (Fig. 5A and B, additional low magnification images provided as Supplementary material). However, in cells treated with **6-PNA1**, there was a significant reduction in the percentage of cells with nuclear immunoreactivity to CHOP compared to DMSO-treated cells (25%, p <0.001), demonstrating that **6-PNA1** is protective against ER stress induced by mutant SOD1 A4V. Similarly, BMC treatment was also protective against induction of UPR: the percentage of transfected cells with CHOP activation was significantly decreased in this cell population (30%, p <0.05).

PNA1 also significantly reduced CHOP activation, to only 26% transfected cells (p <0.05) compared to DMSO-treated cells (37%) (Fig. 5A and C). In contrast, treatment with the negative control PNA, **PNA2**, did not alter the percentage of cells with CHOP activation (40%) and hence ER stress. Treatment of cells with the remaining PNA oligomers (**7-PNA1**, **8-PNA1** and **9-PNA1**) significantly reduced the percentage of transfected cells with ER stress when compared with cells treated with **PNA2** (31%, all p <0.05). However this was not statistically significant when compared with cells treated with DMSO only. As expected, very few untransfected cells (UTR) displayed CHOP up-regulation. Hence these results reveal

Table 1
Thermodynamic data of duplex formation by UVM[a,b]

Duplex	T_m (°C)	$\Delta H°VH$ (kJ mol^{-1})	$\delta\Delta H$	$\Delta G°VH$ (kJ mol^{-1})[c]	$\delta\Delta G$[c]
PNA1/**PNA2**	64 (±1)	−202 (±6)		−14.1 (±1.7)	
6-PNA1/**PNA2**	66 (±1)	−123 (±5)	+79	−7.8 (±1.9)	+6.3
PNA1/DNA[d]	57 (±1)	−183 (±13)		−9.6 (±2.4)	
6-PNA1/DNA[d]	55 (±1)	−106 (±1)	+77	−6.6 (±0.5)	+3.0

[a] Values obtained are an average of a minimum of 3 experiments.
[b] Error corresponds to ±1 standard deviation.
[c] T = 310 K,
[d] DNA sequence used is 5′-AAGTCGTGC-3′.

Table 2
Thermodynamic data of duplex formation by ITC[a,b]

Duplex	$\Delta H°_b$ (kJ mol^{-1})	$\delta\Delta H$	$\Delta G°_b$ (kJ mol^{-1})[c]	$\delta\Delta G$[c]
PNA1/**PNA2**	−216 (±4)		−48.9 (±0.7)	
6-PNA1/**PNA2**	−143 (±3)	+73	−42.7 (±2.8)	+6.2
PNA1/DNA[d]	−169 (±1)		−48.4 (±3.2)	
6-PNA1/DNA[d]	−107 (±1)	+62	−41.8 (±0.5)	+6.6

[a] Values obtained are an average of a minimum of 3 experiments.
[b] Error corresponds to ±1 standard deviation.
[c] T = 310 K.
[d] DNA sequence used is 5′-AAGTCGTGC-3′.

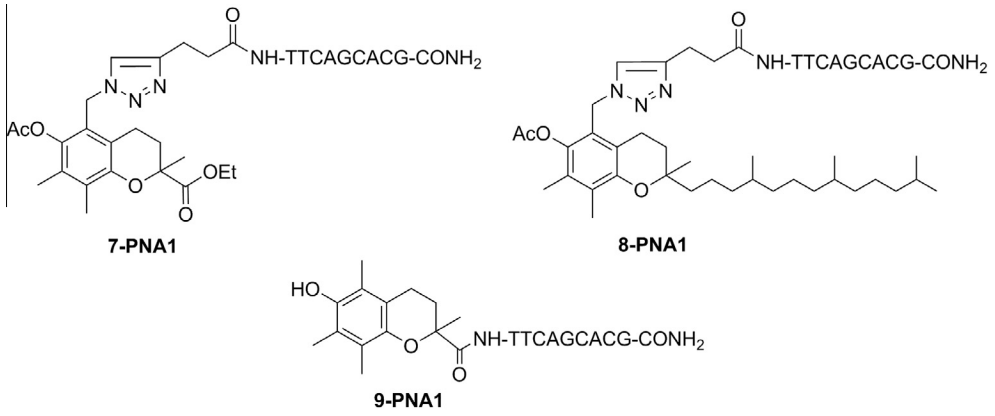

Figure 3. Conjugated vitamin E derived-PNA oligomers.[21]

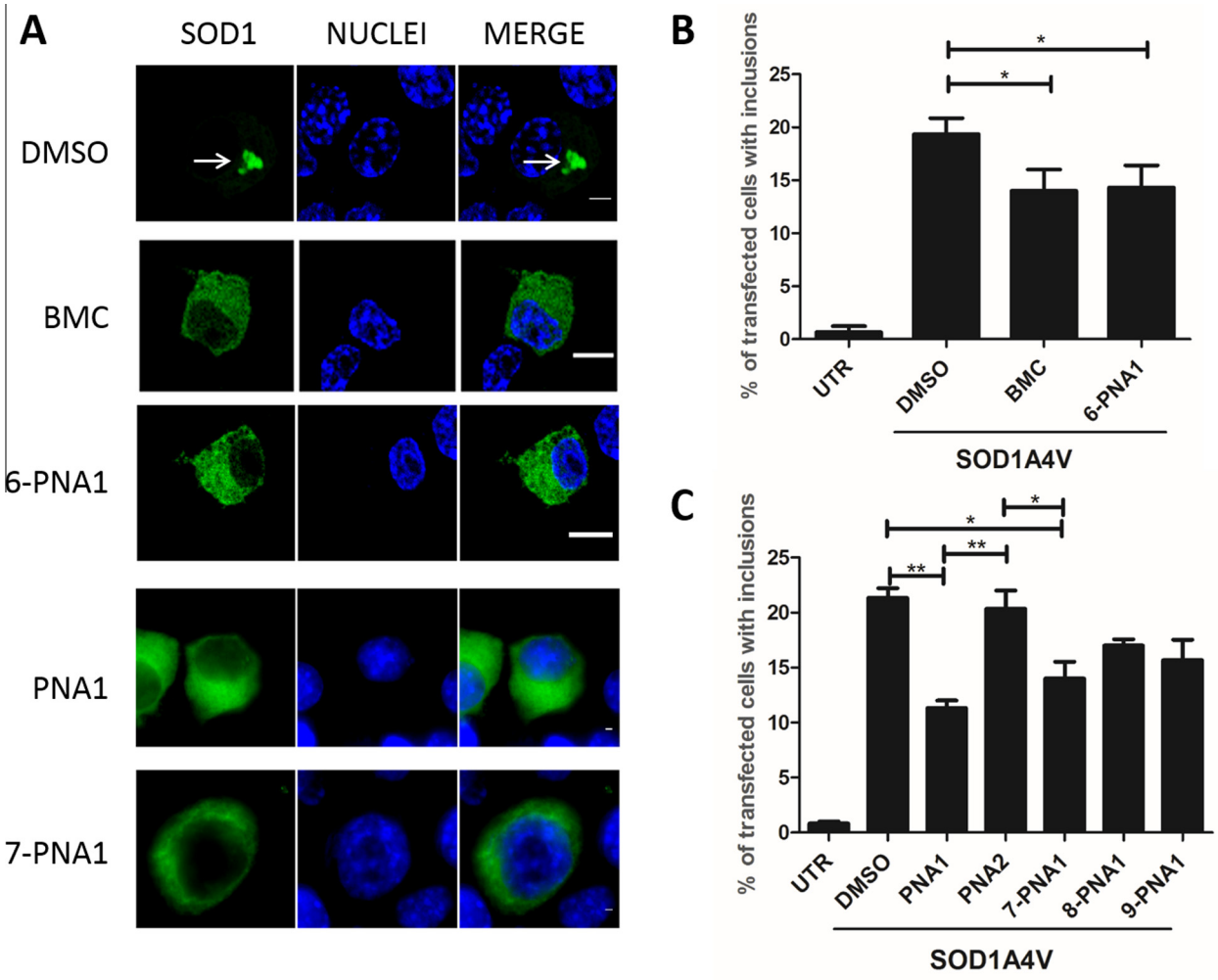

Figure 4. PNA1, **6-PNA1** and **7-PNA1** reduce mutant SOD1 A4V inclusion formation. Fewer mutant SOD1 A4V inclusions are formed in Neuro2a cells treated with PNA compared to cells only treated with DMSO. (A) Fluorescent microscopy images of mutant SOD1 A4V-EGFP expressing in Neuro2a cells at 72 h post transfection. White arrow indicates fluorescent green SOD1 inclusions, shown in first column. Nuclei are shown by Hoechst staining (blue, second column). Merge (third column) represents the combined images from first and second columns. Top panel indicates cells treated with DMSO alone, second panel, BMC treated cells and third panel, **6-PNA1** treated cells. The fourth and the fifth panels represent cells administered with **PNA1** and **7-PNA1**. Scale bar represents 10 μm. (B) Quantification of the percentage of cells bearing SOD1 A4V inclusions in BMC (positive control) and **6-PNA1** treated cells compared to DMSO-only treated cells. (C) Quantification of percentage of cells bearing SOD1 A4V inclusions in PNA treated cells compared to DMSO-only treated cells. In each cell population, 100 transfected cells were examined for the presence of fluorescent green inclusions. UTR represent control, untransfected cells. Data represented as Mean ± SD, $n = 3$, $^{*}p < .05$ $^{**}p < .01$ versus respective controls by one way ANOVA with Tukey's post hoc test.

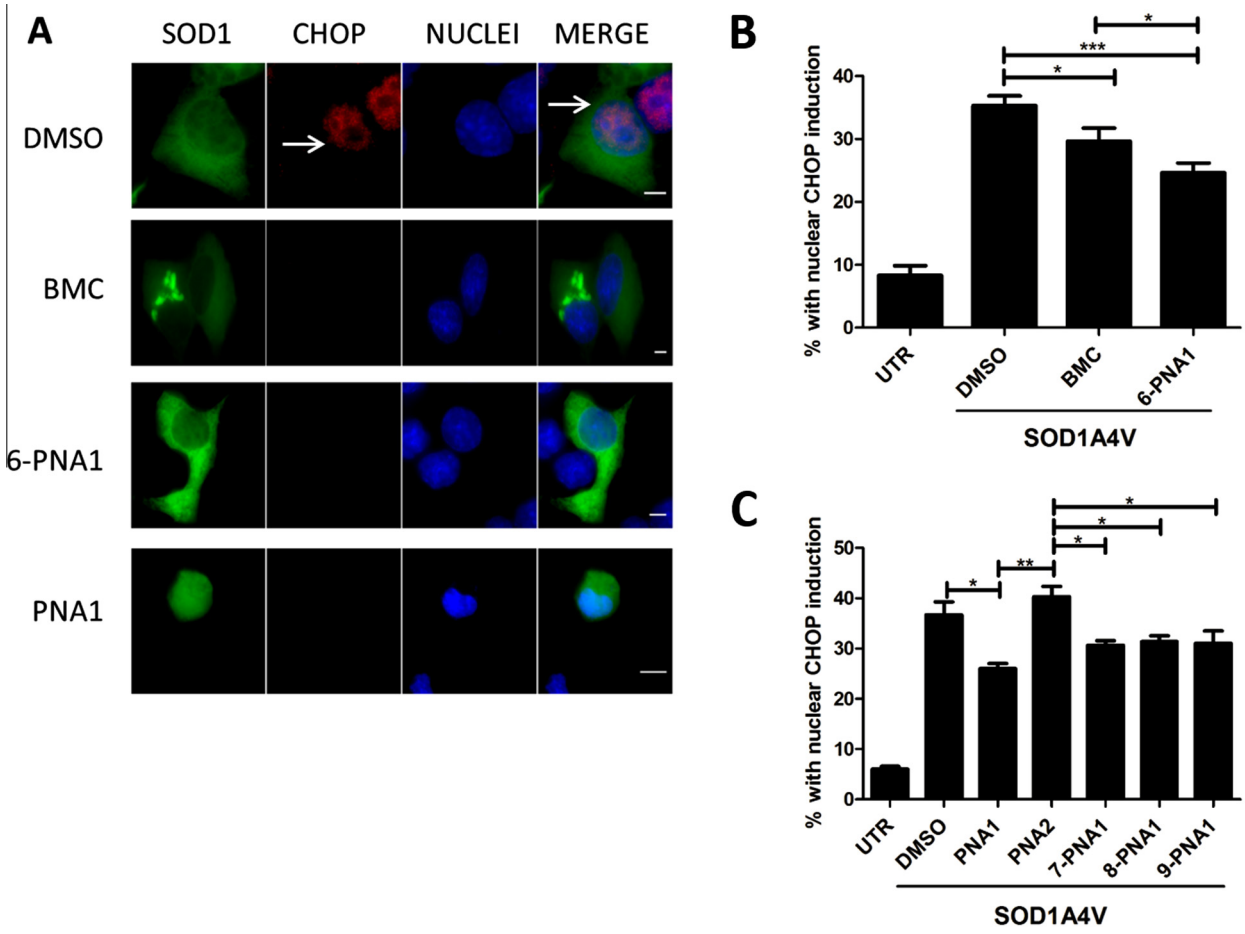

Figure 5. PNA1 and 6-PNA1 reduce activation of CHOP, and hence pro-apoptotic phases of UPR, in cells expressing mutant SOD1. Immunocytochemistry for CHOP was performed in Neuro2a cells expressing mutant SOD1 A4V at 72 h post transfection (A) Fluorescent microscopy images of mutant SOD1 A4V-EGFP transfected Neuro2a cells. White arrow indicates nuclear immunoreactivity to CHOP, indicating its activation, and hence induction of pro-apoptotic phases of UPR in these cells. Fluorescent mutant SOD1 A4V (green) is shown in the first column, immunofluorescence detection of CHOP (red) in the second column, nuclei are shown by Hoechst staining (blue) in the third column, and the fourth column represents merge image of all three. Top panel indicates cells treated with DMSO alone, second panel, BMC treated cells, third panel, **6-PNA1** treated cells, and the fourth panel represents cells administered with **PNA1**. Scale bar represents 10 μm. (B) Quantification of the percentage of cells with nuclear immunoreactivity to CHOP in BMC (positive control) and **6-PNA1** treated cells compared to DMSO-only treated cells. (C) Quantification of the percentage of cells with nuclear immunoreactivity to CHOP in **PNA1**, **7-PNA1**, and **9-PNA1** treated cells compared to either DMSO-only treated cells or negative control PNA (**PNA2**) treated cells. In each cell population, 100 transfected cells were examined for the presence of nuclear CHOP immunoreactivity. UTR represents control, untransfected cells. Data represented as Mean ± SD, $n = 3$, $^{*}p < .05$, $^{**}p < .01$, $^{***}p < .001$ versus respective controls by one way ANOVA with Tukey's post hoc test.

that the PNA compounds **PNA1** and **6-PNA1** were protective against the activation of CHOP, and hence induction of the pro-apoptotic phases of the UPR, in neuronal cells expressing mutant SOD1.

3. Conclusions

The synthesis of a menadione-PNA conjugate was carried out to facilitate thermodynamic studies by both UVM and ITC, which resulted in the formation of the expected duplex indicating thermodynamic stability. Cellular studies were then carried out on both unconjugated and conjugated PNA. We have shown for the first time that compounds containing the peptide nucleic acid sequence of H-GCACGACTT-NH_2 are effective against specific cellular signaling pathways, which complements earlier studies investigating the disease parameters in SOD1 mice but which did not look any further at the specific mechanisms involved. The synthesized PNA oligomers have demonstrated efficacy in reducing mutant SOD1 inclusion formation and ER stress, which are two key cellular pathological hallmarks in ALS, with the unconjugated **PNA1** and the menadione-conjugate **6-PNA1** found to be equally effective. While the conjugation of vitamin K did not strengthen the cellular effects over those observed by the unconjugated PNA, this work has shown that conjugation which is not detrimental to activity is possible and provides an important proof of concept in developing other conjugates. Further studies will be necessary to investigate any benefits vitamin K conjugation may have on the delivery of PNA in an animal model.

4. Experimental

4.1. Synthesis

NMR spectra were recorded on a Bruker Avance-300 Spectrophotometer (1H at 300.13 MHz and 13C at 75.47 MHz) or a Bruker Avance-400 spectrometer (1H at 400.13 MHz and 13C at 100.62 MHz). All PNA and PNA conjugates were analyzed by Matrix Assisted Desorption Ionization Time of Flight mass spectrometry (MALDI-TOF-MS) using an Ultraflex III instrument (Bruker Daltonics, Germany) and α-cyano-4-hydroxy cinnamic acid as the matrix. Electrospray ionization (ESI) mass spectrometry was carried out using an Esquire^{6000} ion trap mass spectrometer (Bruker Daltonics,

Germany). The samples were introduced at a flow rate of 4 μL/min and a mass range of 50 – 3000 *m*/*z* was recorded. A scan rate of 5500 *m*/*z*/*second* was used with the temperature set at 300 °C. The molecular ion peaks (*m*/*z*) were denoted $[M+H]^+$. TLC was performed using Merck Kieselgel 60 F_{254} plates. Drying and purification methods for solvents and reagents were followed by directions from Armarego and Chai.[31] Melting points were collected on hot stage Reichert 'Thermopan' apparatus. The DNA sequence used in the thermodynamic experiments was purchased from Sigma Aldrich.

4.1.1. 2-Methyl-3-bromo-1,4-napthoquinone 1

The synthesis of this compound was based on the method of Teeter et al.[23] Menadione (5.5 g, 31.94 mmol), glacial acetic acid (50 mL) and sodium acetate (11 g, 134.09 mmol) were heated in a conical flask until the suspension dissolved. To this, bromine (2 mL) was added and the flask was stoppered and placed in darkness for 3 days. Water (300 mL) was added and the resulting solid filtered, followed by recrystallisation from methanol to afford the brominated product **1** as bright yellow crystals (5.86 g, 73%), mp 150–152 °C (lit.[23] 151–152 °C). δ_H (300 MHz, $CDCl_3$): 8.15–8.09 (2H, m, Ar*H*), 7.76–7.69 (2H, m, Ar*H*), 2.38 (3H, s, ArCH_3). δ_C (75 MHz, $CDCl_3$): 181.9, 171.5, 148.5, 139.0, 134.1, 133.9, 131.6, 131.2, 127.5, 127.1, 17.9.

4.1.2. 2-Bromo-3-methyl-1,4-dimethoxynapthelene 2

The synthesis of this compound was adapted from the method of Abell et al.[22] To a stirred solution of **1** (1 g, 3.97 mmol), TBAI (176 mg, 0.48 mmol) in water (3.6 mL) and tetrahydrofuran (10.9 mL), a solution of sodium dithionite (4.16 g, 23.9 mmol) in water (10.9 mL) was added and the reaction stirred for 20 min. To this, a solution of potassium hydroxide (15.8 M, 5.8 mL) was added drop-wise and stirred for a further 5 min, at which time dimethylsulfate (4.5 mL, 47.8 mmol) was then added drop-wise and the reaction was stirred overnight. The product was extracted with CH_2Cl_2 (4 × 50 mL), dried with $MgSO_4$ and solvent removed in vacuo. The orange mass was recrystallized from methanol to afford **2** in 62% yield (2.78 g) as light orange crystals, mp 83–84 °C (lit.[22] 82–84 °C). δ_H (300 MHz, $CDCl_3$): 8.09–8.03 (2H, m, Ar*H*), 7.55–7.45 (2H, m, Ar*H*), 3.96 (3H, s, OCH_3), 3.87 (3H, s, OCH_3), 2.52 (3H, s, ArCH_3). δ_C (75 MHz, $CDCl_3$): 150.5, 149.8, 127.8, 127.6, 127.3, 126.5, 126.2, 122.4, 122.4, 117.2, 61.6, 61.3, 16.7.

4.1.3. Ethyl 2-(3-methyl-1,4-dimethoxynapthalen-2-yl)acetate 3

To a cooled solution of **2** (1.96 g, 6.97 mmol) in anhydrous ether (12 mL) under an atmosphere of argon, *n*-butyllithium (1.6 M in hexane, 5.0 mL, 8.02 mmol) was added drop-wise and stirred at 0 °C for 30 min. Copper bromide dimethyl sulfide complex (1.00 g, 4.88 mmol) was added and the solution stirred for 2.5 h. A chilled solution of ethyl bromoacetate (1.16 mL, 10.5 mmol) in ether (8 mL) was then added slowly and the reaction stirred at 0 °C for 2 h, at which time the reaction was warmed to room temperature and stirred for an additional 16 h. The reaction was quenched with 3 M HCl (15 mL) and the two layers were separated. The aqueous layer was extracted with ether (2 × 15 mL) and the combined organic extracts were washed with H_2O (30 mL), saturated aqueous $NaHCO_3$ (30 mL) and once more with H_2O (30 mL). The organic layer was dried with $MgSO_4$ and evaporated in vacuo. The crude orange oil was purified on silica by flash column chromatography, eluting with EtOAc/hexane (1:19) to yield **3** (1.10 g, 55%) as an orange oil. δ_H (300 MHz, $CDCl_3$): 8.06–8.04 (2H, m, Ar*H*), 7.49–7.46 (2H, m, Ar*H*), 4.19 (2H, q, *J* 7.2, OCH_2CH_3), 3.93 (2H, s, ArCH_2), 3.91 (3H, s, OCH_3), 3.86 (3H, s, OCH_3), 2.37 (3H, s, ArCH_3), 1.27 (3H, t, *J* 7.2, OCH$_2CH_3$). δ_C (75 MHz, $CDCl_3$): 171.7, 150.8, 150.1, 128.3, 127.1, 126.7, 126.0, 125.5, 124.1, 122.5, 122.3, 62.2, 61.4, 60.9, 33.1, 14.3, 12.7.

4.1.4. 2-(3-Methyl-1,4-dimethoxynapthelen-2-yl) ethanol 4

The synthesis of this compound was adapted from the method of Abell et al.[22] The ester **3** (873 mg, 3.03 mmol) was vigorously stirred in a solution of anhydrous ether (30 mL) under a bed of argon. To this, $LiAlH_4$ (288 mg, 7.57 mmol) was added and the reaction stirred for 35 min. The reaction was quenched using a saturated solution of aqueous NH_4Cl (10 mL), the two layers were separated and the aqueous layer was extracted with EtOAc (30 mL). The combined organic layers were washed with H_2O (15 mL) followed by brine (15 mL), dried with $MgSO_4$ and the solvent removed in vacuo. The resulting solid was purified on silica by flash column chromatography eluting with EtOAc/hexane (1:4) to afford **4** as an off white solid (692 mg, 93%), mp 68–70 °C (lit.[22] 66–69 °C). δ_H (300 MHz, $CDCl_3$): 8.01–7.99 (2H, m, Ar*H*), 7.46–7.43 (2H, m, Ar*H*), 3.89 (3H, s, OCH_3), 3.85 (3H, s, OCH_3), 3.83 (2H, t, *J* 7.2, CH_2CH_2OH), 3.11 (2H, t, *J* 6.9, ArCH_2CH_2), 2.78 (1H, s (b), *OH*), 2.41 (3H, s, ArCH_3). δ_C (75 MHz, $CDCl_3$): 150.6, 150.3, 127.9, 127.4, 127.0, 126.5, 125.8, 125.5, 122.2, 62.6, 62.0, 61.4, 18.5, 12.6.

4.1.5. 2-(3-Methyl-1,4-dimethoxynaphthalen-2-yl)ethyl hydrogen succinate 5

The synthesis of this compound was adapted from the method of Abell et al.[22] To a stirred solution of alcohol **4** (490 mg, 1.99 mmol) in CH_2Cl_2 (25 mL), a solution of TEA (400 μL, 2.88 mmol), succinic anhydride (420 mg, 4.18 mmol) and DMAP (22 mg, 0.18 mmol) in CH_2Cl_2 (15 mL) was added drop-wise and the reaction stirred overnight. The solvent was removed in vacuo and the resulting residue was dissolved in CH_2Cl_2 (30 mL) and washed with 10% HCl (20 mL) followed by H_2O (2 × 20 mL), dried with $MgSO_4$ and the solvent removed in vacuo to give **5** (680 mg, 98%) as a yellow oil. δ_H (300 MHz, $CDCl_3$): 8.06–7.99 (2H, m, Ar*H*), 7.46–7.44 (2H, m, Ar*H*), 4.28 (2H, t, *J* 7.5, OCH_2CH_2), 3.90 (3H, s, OCH_3), 3.85 (3H, s, *OCH*$_3$), 3.16 (2H, t, *J* 7.2, ArCH_2), 2.93 (1H, s, *OH*), 2.67–2.64 (4H, m, *CH*$_2$*CH*$_2$), 2.44 (3H, s, ArCH_3). δ_C (75 MHz, $CDCl_3$): 178.0, 172.2, 151.0, 150.2, 128.0, 127.1, 126.6, 126.2, 125.9, 125.5, 122.3, 122.2, 64.0, 62.2, 61.3, 28.9, 28.3, 26.7, 12.5.

4.1.6. 2-(3-Methyl-1,4-naphthoquinon-2-yl)ethyl hydrogen succinate 6

The synthesis of this compound was adapted from the method of Abell et al.[22] To a cooled solution of **5** (990 mg, 2.85 mmol), in a 2:1 solution of CH_3CN:H_2O (11 mL), a solution of ceric ammonium nitrate (3.92 g, 7.14 mmol) in 1:1 CH_3CN:H_2O (13 mL) was added drop-wise and the reaction stirred at 0 °C for 30 min, followed by 20 min at room temperature. The solution was diluted with H_2O (50 mL) and the bright yellow solution was extracted with CH_2Cl_2 (6 × 40 mL). The combined organic solution was washed with H_2O (50 mL), dried with $MgSO_4$ and the solvent removed in vacuo to afford **6** as a yellow-orange oil (762 mg, 84%). δ_H (400 MHz, $CDCl_3$): 8.08–8.04 (2H, m, Ar*H*), 7.71–7.67 (2H, m, Ar*H*), 4.28 (2H, t, *J* 6.6, OCH_2), 3.00 (2H, t, *J* 6.6, ArCH_2), 2.65–2.55 (4H, m, *CH*$_2$*CH*$_2$), 2.22 (3H, s, ArCH_3). δ_C (100 MHz, $CDCl_3$): 184.9, 184.3, 177.7, 172.0, 145.5, 142.6, 133.5, 133.5, 132.0, 131.9, 126.3, 63.0, 28.7, 26.7, 13.0.

4.2. PNA synthesis and characterization by UVM and ITC

4.2.1. Synthesis

Bhoc- and Fmoc-protected PNA monomers (A, C, G and T) and 2-aminoethoxy-2-ethoxyacetic acid (AEEA) were purchased from ASM Research Chemicals and were used without further purification. Automated synthesis was performed on an Expedite 8909 nucleic acid synthesizer, on a 2 μmol scale using Fmoc-PAL-PEG-PS resin (0.19 mmol/g) from Applied Biosystems, following the

standard protocols.[24] The synthetic procedure follows a deprotection and coupling strategy using solutions of 0.2 M PNA monomers in *N*-methylpyrrolidone for all monomers except for the C monomer (0.1 M) which was double coupled, deblocking solution (20% piperidine in DMF) then activation using a base solution (0.18 M HATU, 0.2 M DIPEA and 0.3 M 2,6-lutidine in DMF). Capping with 5% v/v acetic anhydride and 6% v/v 2,6-lutidine in DMF terminates incomplete sequences. Conjugates (0.2 M in DMF) were coupled to the PNA oligomer on resin following the same protocol. The PNA was cleaved from the resin using TFA/*m*-cresol (4:1) then precipitated and washed with ice cold ether and dried. The crude PNA was purified using a Phenomenex Jupiter C18 10 μm, 250 mm × 10 mm column, with gradient elution using water (Eluent A) and acetonitrile (Eluent B) with 0.1% TFA. The pure PNA fractions were collected, lyophilized and characterized by MALDI-TOF and ESI mass spectroscopy as appropriate.

4.2.2. Determination of solution concentration

All experiments were carried out in 10 mM sodium phosphate buffer (pH 7.0). The concentrations of both PNA and DNA strands were determined by UV absorption at a wavelength of 260 nm at 80 °C, using quartz cells with a 1 cm path length. The following extinction coefficients were used; εDNA:A = 15300 M^{-1} cm^{-1}, εDNA:G = 12220 M^{-1} cm^{-1}, εDNA:C = 7600 M^{-1} cm^{-1}, εDNA:T = 8700 M^{-1} cm^{-1}, εPNA:A = 13700 M^{-1} cm^{-1}, εPNA:G = 11700 M^{-1} cm^{-1}, εPNA:C = 6600 M^{-1} cm^{-1}, εPNAT = 8600 M^{-1} cm^{-1}.[24]

4.2.3. UV melting experiments

Melting curves were performed on a Varian Cary 100 Bio UV–Vis spectrophotometer with a Cary temperature controller. The duplexes formed during the ITC experiments were used directly to obtain the melting curves, as previously undertaken in the literature.[28] Samples were prepared by heating to 80 °C for 5 min, cooling to 20 °C over 20 min and holding at 20 °C for a further 20 min. The melting curves were measured at 260 nm, with the temperature increasing from 20 °C to 80 °C at a rate of 0.5 °C/min, with data collection occurring every 0.2 °C. Each duplex melting curve was performed in triplicate, at a minimum.

4.2.4. Determination of thermodynamic parameters via UVM

The melting temperature (T_m) is dependent upon α, which is the fraction of the single strand in a duplex state, as described by Marky and Breslaur[25] is shown by Eq. A below:

$$\alpha = \frac{A_s - A}{(A_s - A) + (A - A_d)} \quad \text{(A)}$$

where A is absorbance at a given T, and A_s and A_d are the absorbance from the single strand and the duplex respectively. The T_m of the duplex is determined where α = 0.5.

In order to calculate the van't Hoff enthalpy, the equilibrium constant (K) must be determined and expressed in terms of α for a non-complementary association, as shown in Eq. B, where CT is the total strand concentration and n is the number of strands associated with the complex.

$$K = \frac{\alpha}{(CT/n)^{n-1}(1-\alpha)^n} \quad \text{(B)}$$

Thus, the Gibbs free energy change can be determined (Eq. C) where a plot of ln (K) versus $1/T$ will determine both the enthalpy and entropy of the system (Eqs. D and E, respectively).

$$\Delta G_v H^\circ = -RT\ \ln(K) = \Delta H^\circ - T\Delta S^\circ \quad \text{(C)}$$

$$\Delta H_v H^\circ = \text{slope } (\ln(K) \text{ vs } 1/T)R \quad \text{(D)}$$

$$\Delta S_v H^\circ = \text{intercept } (\ln(K) \text{ vs } 1/T)R \quad \text{(E)}$$

4.2.5. Isothermal titration calorimetry

Calorimetric experiments were performed on a CSC 5300 Nano-ITC 111 instrument at 25 °C, where one of the oligomer strands (~0.1 mM, 100 μL) was titrated into 1.4 mL of the complementary strand (~5 μM). Each injection was 4 or 5 μL at 5 min intervals for a total of 25 injections. Stirrer speed was set to 250 rpm. Solutions were thoroughly degassed by sonification and absolute concentrations determined as outlined above. The reference cell was filled with degassed and deionized water. Isotherms were examined using the software NanoAnalyze v2.0, whereby the binding constant (K_b), intrinsic molar enthalpy change (ΔH_b°) and stoichiometry of binding (n) were determined by means of best fit (independent model) of the calorimetric data. The data was corrected by subtracting the heat of dilution from the experiment. Each duplex was titrated in triplicate, at a minimum.

4.3. Cellular biology

4.3.1. Constructs and cell lines

The mouse neuroblastoma Neuro-2a cell line (ATCC cell line CCL-131) was used for all transient transfections. The SOD1A4V-EGFP construct was as described previously.[30]

4.3.2. Cell culture and transfection

Neuro2a cells were maintained in Dulbecco modified Eagle's medium with 10% fetal calf serum, 100 mg/ml penicillin and 100 mg/ml streptomycin. Transfections were performed using Lipofectamine reagent 2000 (Invitrogen) according to the manufacturer's protocol. Cells transfected with SOD1A4V-EGFP were examined 72 h post-transfection by fluorescence microscopy and cells with prominent EGFP-positive inclusions were counted as a percentage of the total EGFP-positive, and hence transfected, cells. Treatment with PNA derivatives were added from a stock dissolved at 25 μM in DMSO. (+/−)-*trans*-1,2-bis(2-mercaptoacetamido)cyclohexane (BMC) (25 μM in DMSO) was also added to the transfected cell expressing SOD1 as a positive control, 4 h post transfection cells were analyzed for inclusion positive cells and ER stress as previously described.[13]

4.3.3. Immunofluorescence and microscopy

Cells were fixed with freshly prepared 4% (w/v) paraformaldehyde and incubated in the dark for 15 min. The cells were permeabilized with 0.2% (v/v) Triton-X in PBS for 5 min and blocked with 3% BSA in PBS for 30 min. After washing with 0.1% (v/v) Tween-20 in PBS, incubation with mouse anti-CHOP (1:50) (Abcam) antibody was performed in PBS at 4 °C overnight. The secondary antibody, AlexaFluor 568 conjugated rabbit anti-mouse IgG (1:250), was added for 1 h and incubated in the dark at room temperature. After washing, staining of nuclei was performed with Hoechst stain 33342 (Invitrogen) and mounted using fluorescent mounting media. The slides were observed under 100× magnification on an Olympus epifluorescent microscope. DAPI (nuclei), FITC (GFP fluorescence) filters were used for viewing and images taken using NIS-Elements BR 3.2 software.

4.3.4. Statistics

Cells transfected with SOD1-EGFP were counted (100 total) and the data was represented as Mean ± SD. Analyses were made using ANOVA followed by Tukey's post hoc test. (GraphPad Prism, San Diego, CA, USA). p-Values of 0.05 or less were considered significant. p <0.05*, p <0.01**, p <0.001***.

Acknowledgments

This work was supported by an Australian Research Council Discovery Project (DP0771578). E.C.B. is a recipient of an Aus-

tralian Postgraduate Award and LIMS Postgraduate Writing-Up Award. S.P. holds a La Trobe University Postgraduate Research Scholarship and a Macquarie University Postgraduate Research Scholarship.

Supplementary data

Supplementary data associated with this article can be found, in the online version, at http://dx.doi.org/10.1016/j.bmc.2016.02.022.

References and notes

1. Rosenfeld, J.; Strong, M. J. *Neurotherapeutics* **2015**, *12*, 317.
2. Rowland, L. P.; Shneider, N. A. *N. Engl. J. Med.* **2001**, *344*, 1688.
3. Rosen, D. R.; Siddique, T.; Patterson, D.; Figlewicz, D. A.; Sapp, P.; Hentati, A.; Donaldson, D.; Goto, J.; O'Regan, J. P.; Deng, H.-X.; Rahmani, Z.; Krizus, A.; McKenna-Yasek, D.; Cayabyab, A.; Gaston, S. M.; Berger, R.; Tanzi, R. E.; Halperin, J. J.; Herzfeldt, B.; Van den Bergh, R.; Hung, W.-Y.; Bird, T.; Deng, G.; Mulder, D. W.; Smyth, C.; Laing, N. G.; Soriano, E.; Pericak-Vance, M. A.; Haines, J.; Rouleau, G. A.; Gusella, J. S.; Horvitz, H. R.; Brown, R. H. *Nature* **1993**, *362*, 59.
4. Cudkowicz, M. E.; McKenna-Yasek, D.; Sapp, P. E.; Chin, W.; Geller, B.; Hayden, D. L.; Schoenfeld, D. A.; Hosler, B. A.; Horvitz, H. R.; Brown, R. H. *Ann. Neurol.* **1997**, *41*, 210.
5. Keerthana, S.; Kolandaivel, P. *J. Biomol. Struct. Dyn.* **2015**, *33*, 167.
6. Bosco, D. A.; Morfini, G.; Karabacak, N. M.; Song, Y.; Gros-Louis, F.; Pasinelli, P.; Goolsby, H.; Fontaine, B. A.; Lemay, N.; McKenna-Yasek, D.; Frosch, M. P.; Agar, J. N.; Julien, J. P.; Brady, S. T.; Brown, R. H., Jr. *Nat. Neurosci.* **2010**, *13*, 1396.
7. Brujin, L. I.; Houseweart, M. K.; Kato, S.; Anderson, K. L.; Anderson, S. D.; Ohama, E.; Reaume, A. G.; Scott, R. W.; Cleveland, D. W. *Science* **1998**, *281*, 1851.
8. Oyadomari, S.; Mori, M. *Cell Death Differ.* **2004**, *11*, 381.
9. Atkin, J. D.; Farg, M. A.; Walker, A. K.; McLean, C.; Tomas, D.; Horne, M. K. *Neurobiol. Dis.* **2008**, *30*, 400.
10. Atkin, J. D.; Farg, M. A.; Turner, B. J.; Tomas, D.; Lysaght, J. A.; Nunan, J.; Rembach, A.; Nagley, P.; Beart, P. M.; Cheema, S. S.; Horne, M. K. *J. Biol. Chem.* **2006**, *281*, 30152.
11. Saxena, S.; Cabuy, E.; Caroni, P. *Nat. Neurosci.* **2009**, *12*, 627.
12. Saxena, S.; Roselli, F.; Singh, K.; Leptien, K.; Julien, J. P.; Gros-Louis, F.; Caroni, P. *Neuron* **2013**, *80*, 80.
13. Walker, A. K.; Farg, M. A.; Bye, C. R.; McLean, C. A.; Horne, M. K.; Atkin, J. D. *Brain* **2010**, *133*, 105.
14. Atkin, J. D.; Farg, M. A.; Soo, K. Y.; Walker, A. K.; Halloran, M.; Turner, B. J.; Nagley, P.; Horne, M. K. *J. Neurochem.* **2014**, *129*, 190.
15. Dean, D. A. *Adv. Drug Delivery Rev.* **2000**, *44*, 81.
16. Hamilton, S. E.; Iyer, M.; Norton, J. C.; Corey, D. R. *Bioorg. Med. Chem. Lett.* **1996**, *6*, 2897.
17. Tsaioun, K. I. *Nutr. Rev.* **1999**, *57*, 231.
18. Thijssen, H. H. W.; Vervoort, L. M. T.; Schurgers, L. J.; Shearer, M. J. *Brit. J. Nutri.* **2006**, *95*, 260.
19. Gildea, B. D.; Casey, S.; MacNeill, J.; Perry-O'Keefe, H.; Sørensen, D.; Coull, J. M. *Tetrahedron Lett.* **1998**, *39*, 7255.
20. Manor, D.; Morley, S. *Vitamin E*; Academic Press: U.S.A., 2007. Vol. 76, pp 46–60.
21. Browne, E. C.; Langford, S. J.; Abbott, B. M. *Org. Biomol. Chem* **2013**, *11*, 6744.
22. Payne, R. J.; Daines, A. M.; Clark, B. M.; Abell, A. D. *Bioorg. Med. Chem.* **2004**, *12*, 5785.
23. Adams, R.; Geissman, T. A.; Baker, B. R.; Teeter, H. M. *J. Am. Chem. Soc.* **1941**, *63*, 528.
24. Braasch, D. A.; Corey, D. R. *Methods* **2001**, *23*, 97.
25. Marky, L. A.; Breslauer, K. J. *Biopolymers* **1987**, *26*, 1601.
26. Wartell, R. M.; Benight, A. S. *Phys. Rep.* **1985**, *126*, 67.
27. Ghai, R.; Falconer, R. K.; Collins, B. M. *J. Mol. Recognit.* **2011**, *25*, 32.
28. Chakrabarti, M. C.; Schwarz, F. P. *Nucleic Acids Res.* **1999**, *27*, 4801.
29. Jensen, K. K.; Orum, H.; Nielsen, P. E.; Nordén, B. *Biochemistry* **1997**, *36*, 5072.
30. Turner, B. J.; Atkin, J. D.; Farg, M. A.; Zang, D. W.; Rembach, A.; Lopes, E. C.; Patch, J. D.; Hill, A. F.; Cheema, S. S. *J. Neurosci.* **2005**, *25*, 108.
31. Armarego, W. L. F.; Chai, C. L. L. *Purification of Laboratory Chemicals*, 5th ed.; Elsevier, 2003.